

## RNA Conformation in Catalytically Active Human Telomerase

Justin A. Yeoman,<sup>†,§</sup> Angel Orte,<sup>†,||</sup> Beth Ashbridge,<sup>†</sup> David Klenerman,<sup>\*,†</sup> and Shankar Balasubramanian<sup>\*,†,‡</sup>

*The University Chemical Laboratory, University of Cambridge, Lensfield Road, Cambridge CB2 1EW, U.K., and School of Clinical Medicine, University of Cambridge, Cambridge CB2 0SP, U.K.*

Received November 5, 2009; E-mail: dk10012@cam.ac.uk; sb10031@cam.ac.uk

Telomerase is the specialized reverse transcriptase responsible for DNA synthesis at chromosomal termini.<sup>1</sup> The two core components of human telomerase that are essential for catalytic activity are human telomerase RNA (hTR)<sup>2</sup> and human telomerase reverse transcriptase (hTERT).<sup>3</sup> hTR contains the template for reverse transcription and acts as a scaffold for assembly of the telomerase holoenzyme. Two regions of the hTR primary sequence that are conserved among vertebrates, CR2 and CR3, are predicted to fold into a type of structure called a pseudoknot, in which the single-stranded terminal loop of an RNA stem–loop is base-paired with a single-stranded region elsewhere in the RNA molecule.<sup>4</sup> The presence of a pseudoknot element in close proximity to the template, within a template/pseudoknot domain, has been proposed as a universal feature of telomerase RNAs from all species.<sup>5</sup> Conservation of this motif is suggestive of an important role in telomerase function, and this has been supported by mutational analysis.<sup>6–9</sup> A minimal but nonfunctional model of the hTR pseudoknot, ~50 nucleotides in length and formed essentially from sequences CR2 and CR3 alone, does fold into a pseudoknot.<sup>8,10–13</sup> However, there is a lack of direct physical evidence to support the existence of a pseudoknot in full-length wild-type (wt) telomerase RNA from humans or any other species. Herein we provide biophysical evidence to support the existence of a pseudoknot in full-length hTR, but only as part of a catalytically competent telomerase complex.

For our studies, we first synthesized a dual-labeled full-length hTR construct, **DL hTR**, that was site-specifically modified with a donor and an acceptor fluorophore suitable for Förster resonance energy transfer (FRET) analysis specifically to report on pseudoknot formation (Figure 1). In particular, formation of helix P3 and therefore the hTR pseudoknot was predicted, on the basis of an NMR structure of the minimal wt hTR pseudoknot and a molecular model of the entire template/pseudoknot domain, to result in formation of a high-FRET species (FRET efficiency close to 0.68) (Figure 1a; for details of the interfluorophore distance calculation, see the Supporting Information).<sup>13,14</sup> A scenario in which the hTR pseudoknot was not present was predicted to result in formation of a low- or zero-FRET species (Figure 1b). We assembled **DL hTR** from three pieces of RNA; two were generated by runoff in vitro transcription, and the third was produced by chemical synthesis. **DL hTR** was prepared by enzymatic DNA-splinted RNA ligation from three hTR fragments in one step (see the Supporting Information).

Because of the low quantities of sample we were able to produce, which precluded classical ensemble biophysical approaches, and

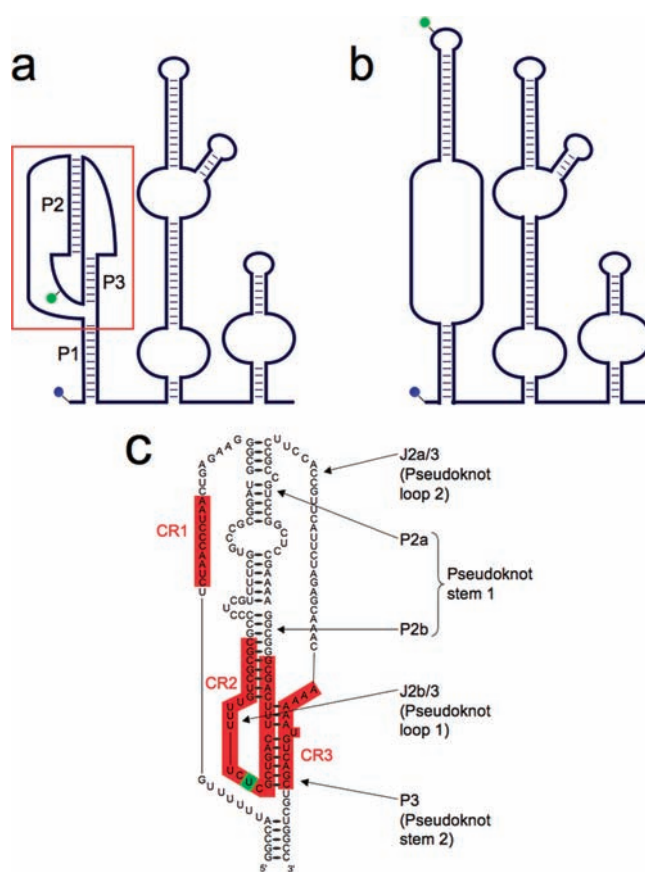


**Figure 1.** Structure of **DL hTR**. The positions of fluorophores Alexa Fluor 488 (blue) and Alexa Fluor 594 (green) are indicated. (a) Overall secondary structure. Helices P1–3 are labeled, and the pseudoknot is boxed. In this case, the fluorophores are close enough to produce a high-FRET signal. (b) Alternative hairpin conformation. In this case, a low- or zero-FRET signal is expected. (c) Detailed view of the hTR pseudoknot. Conserved regions CR1–3 and the pseudoknot stems and loops are labeled.

the potential for conformational heterogeneity, it was advantageous to study **DL hTR** at the single-molecule level to establish the conformation of the hTR template/pseudoknot domain. As a result of donor fluorophore photophysical effects, a peak centered at zero FRET efficiency is ubiquitous in conventional single-pair FRET experiments.<sup>15</sup> In order to avoid this zero-FRET peak and the variations in detection efficiencies of populations with different degrees of energy transfer, the technique known as two-color coincidence detection with single excitation (TCCD-1ex) was employed.<sup>15</sup> TCCD-1ex is based on an AND threshold and has been shown to determine accurately the relative populations of different FRET species. In this case, three independent measurements involving two different RNA preparations were performed.

<sup>†</sup> The University Chemical Laboratory.

<sup>‡</sup> School of Clinical Medicine.

<sup>§</sup> Current address: National Centre for Biological Sciences, Tata Institute of Fundamental Research, UAS GKVK, Bellary Road, Bangalore 560 065, India.

<sup>||</sup> Current address: Department of Physical Chemistry, Faculty of Pharmacy, Campus Cartuja, Granada 18071, Spain.

Purified **DL hTR** in solution reproducibly displayed two populations, centered around  $-1.50$  and  $-0.25$  on the TCCD scale (Figure 2a), which represent apparent FRET efficiencies of 0.18 and 0.44 after conversion to the conventional FRET scale (see the Supporting Information). These two populations are consistent with two extended conformations of the template/pseudoknot domain in which a pseudoknot is not formed. Bulk analysis of the donor and acceptor lifetimes in **DL hTR** showed that the FRET signals for the two populations were due to genuine differences in energy transfer efficiency from donor to acceptor, as opposed to quenching effects caused by the fluorophore microenvironment (see the Supporting Information).

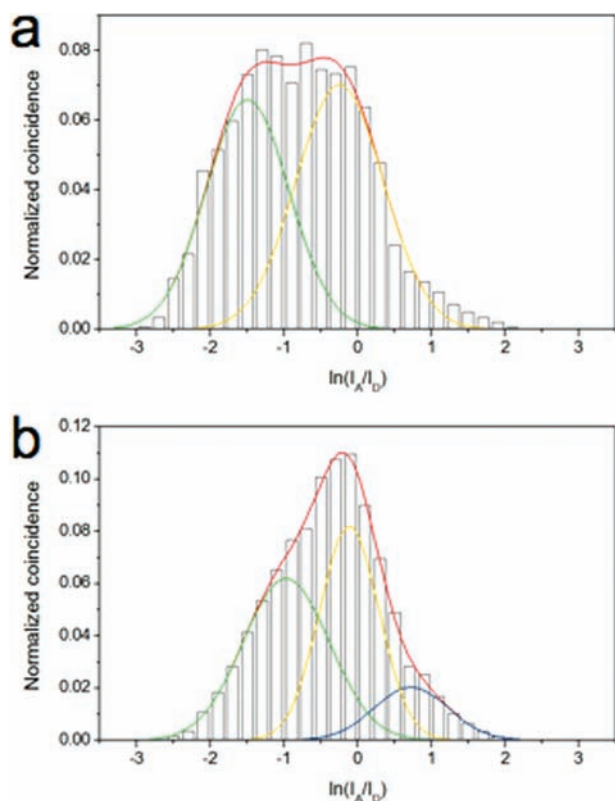


**Figure 2.** Representative examples of two-color coincidence detection (TCCD) histograms for (a) **DL hTR** and (b) **DL hTR**·hTERT. The fitted FRET subpopulations are shown.

We then expressed hTERT in the presence of the dual-labeled hTR to assess the effect of **DL hTR**·hTERT complex formation on RNA pseudoknot folding. The resulting complex was catalytically active (see the Supporting Information). **DL hTR** complexed with hTERT was observed at the single-molecule level to establish the conformation of the hTR template/pseudoknot domain in active human telomerase. Three independent measurements were performed. Two populations were observed at positions comparable to those observed for **DL hTR** alone (green and yellow Gaussian peaks in Figure 2b), indicative of uncomplexed **DL hTR**. A third population with a high FRET efficiency was observed around  $+0.73$  on the TCCD scale (blue Gaussian peak in Figure 2b), indicative of **DL hTR**·hTERT complex. The apparent FRET efficiency of the third peak was 0.67, and this species formed on average  $9.3 \pm 3.3\%$  of the detectable population. The appearance of a high-FRET population (FRET efficiency close to 0.68) indicated that assembly with hTERT alters the conformation of hTR and is consistent with

formation of an RNA pseudoknot. However, we cannot rule out the possibility that the new FRET population is due to an alternative nonpseudoknot RNA conformation. The validity of the addition of a third peak in the fitting was supported by a large decrease in the reduced  $\chi^2$  value as well as by  $F$  tests to compare fits of two versus three Gaussian peaks. Both criteria showed that the best fit for the **DL hTR**·hTERT sample was obtained using three peaks, whereas the best fit for **DL hTR** in the absence of hTERT was obtained with two peaks (see the Supporting Information). Additional bulk FRET and time-resolved fluorescence data support the conclusion that the differences in **DL hTR** FRET efficiency arose from actual differences in interfluorophore distance (see the Supporting Information).

hTERT might induce hTR pseudoknot formation on binding, or alternatively, hTR in solution might transiently adopt a pseudoknot structure that may be bound and stabilized by hTERT. The relatively low proportion of **DL hTR** molecules exhibiting such high FRET can be related to the relatively low efficiency of in vitro telomerase reconstitution. Indeed, we have previously observed that after purification, 12–15% hTR·hTERT complex is present with an excess of uncomplexed hTR and hTERT molecules.<sup>16</sup> The  $9.3 \pm 3.3\%$  size of the high-FRET subpopulation lies in the range expected for the **DL hTR**·hTERT complex, considering that peaks of high FRET efficiency are detected 40% less effectively than peaks in the mid-FRET range.<sup>15</sup>

These data provide the first direct physical evidence in support of pseudoknot formation in full-length hTR. The study suggests that the hTR pseudoknot is stable only when hTR is complexed with hTERT to form a catalytically active telomerase ribonucleoprotein.

**Acknowledgment.** We thank Mariana Mihalusova of the Zhuang group, Harvard, for valuable advice. We thank the BBSRC for financial assistance, and A.O. thanks the Sixth EU Framework Programme for a Marie Curie Intra-European Fellowship.

**Supporting Information Available:** General experimental protocols, experimental details for the synthesis of **DL hTR**, experimental details and data for the TRAP assay, details of the interfluorophore distance calculation, and additional FRET data. This material is available free of charge via the Internet at <http://pubs.acs.org>.

## References

- Greider, C.; Blackburn, E. *Cell* **1985**, *43*, 405–413.
- Feng, J.; Funk, W.; Wang, S.; Weinrich, S.; Avilion, A.; Chiu, C.; Adams, R.; Chang, E.; Allsopp, R.; Yu, J. *Science* **1995**, *269*, 1236–1241.
- Nakamura, T.; Morin, G.; Chapman, K.; Weinrich, S.; Andrews, W.; Lingner, J.; Harley, C.; Cech, T. *Science* **1997**, *277*, 955–959.
- Chen, J.; Blasco, M.; Greider, C. *Cell* **2000**, *100*, 503–514.
- Lin, J.; Ly, H.; Hussain, A.; Abraham, M.; Pearl, S.; Tzfati, Y.; Parslow, T.; Blackburn, E. *Proc. Natl. Acad. Sci. U.S.A.* **2004**, *101*, 14713–14718.
- Comolli, L.; Smirnov, I.; Xu, L.; Blackburn, E.; James, T. *Proc. Natl. Acad. Sci. U.S.A.* **2002**, *99*, 16998–17003.
- Ly, H.; Xu, L.; Rivera, M.; Parslow, T.; Blackburn, E. *Genes Dev.* **2003**, *17*, 1078–1083.
- Theimer, C.; Blois, C.; Feigon, J. *Mol. Cell* **2005**, *17*, 671–682.
- Chen, J.; Greider, C. *Proc. Natl. Acad. Sci. U.S.A.* **2005**, *102*, 8080–8085.
- Theimer, C.; Finger, L.; Trantirek, L.; Feigon, J. *Proc. Natl. Acad. Sci. U.S.A.* **2003**, *100*, 449–454.
- Yingling, Y.; Shapiro, B. *J. Mol. Graphics Modell.* **2006**, *25*, 261–274.
- Chen, G.; Wen, J.-D.; Tinoco, I., Jr. *RNA* **2007**, *13*, 1–14.
- Kim, N.-K.; Zhang, Q.; Zhou, J.; Theimer, C. A.; Peterson, R. D.; Feigon, J. *J. Mol. Biol.* **2008**, *384*, 1249–1261.
- Gavory, G.; Symmons, M. F.; Ghosh, Y. K.; Klenerman, D.; Balasubramanian, S. *Biochemistry* **2006**, *45*, 13304–13311.
- Orte, A.; Clarke, R.; Klenerman, D. *Anal. Chem.* **2008**, *80*, 8389–8397.
- Alves, D.; Li, H.; Codrington, R.; Orte, A.; Ren, X.; Klenerman, D.; Balasubramanian, S. *Nat. Chem. Biol.* **2008**, *4*, 287–289.

JA909383N